



# Optogenetic activation of corticogeniculate feedback stabilizes response gain and increases information coding in LGN neurons

Allison J. Murphy<sup>1,2</sup> · Luke Shaw<sup>1</sup> · J. Michael Hasse<sup>3,4</sup> · Robbe L. T. Goris<sup>5,6</sup> · Farran Briggs<sup>1,2,3,7,8</sup>

Received: 16 February 2020 / Revised: 10 June 2020 / Accepted: 24 June 2020 / Published online: 6 July 2020  
© Springer Science+Business Media, LLC, part of Springer Nature 2020

## Abstract

In spite of their anatomical robustness, it has been difficult to establish the functional role of corticogeniculate circuits connecting primary visual cortex with the lateral geniculate nucleus of the thalamus (LGN) in the feedback direction. Growing evidence suggests that corticogeniculate feedback does not directly shape the spatial receptive field properties of LGN neurons, but rather regulates the timing and precision of LGN responses and the information coding capacity of LGN neurons. We propose that corticogeniculate feedback specifically stabilizes the response gain of LGN neurons, thereby increasing their information coding capacity. Inspired by early work by McClurkin et al. (1994), we manipulated the activity of corticogeniculate neurons to test this hypothesis. We used optogenetic methods to selectively and reversibly enhance the activity of corticogeniculate neurons in anesthetized ferrets while recording responses of LGN neurons to drifting gratings and white noise stimuli. We found that optogenetic activation of corticogeniculate feedback systematically reduced LGN gain variability and increased information coding capacity among LGN neurons. Optogenetic activation of corticogeniculate neurons generated similar increases in information encoded in LGN responses to drifting gratings and white noise stimuli. Together, these findings suggest that the influence of corticogeniculate feedback on LGN response precision and information coding capacity could be mediated through reductions in gain variability.

**Keywords** LGN · Corticogeniculate · V1 · Optogenetics · Variance · Entropy

## 1 Introduction

The first feedback step in the visual system is the corticogeniculate (CG) pathway that links the primary visual cortex (V1) with the dorsal lateral geniculate nucleus of the thalamus (LGN; Sherman and Guillery 2006). Although CG synapses onto LGN relay neurons far outnumber synapses from retinal ganglion cells (Erisir et al. 1997a; Erisir et al. 1997b), LGN neurons derive their spatial receptive field

properties from their retinal rather than their cortical inputs (Usrey et al. 1999). Accordingly, CG inputs “modulate” rather than “drive” visual responses in LGN neurons (Sherman and Guillery 1998), although the functional role of this modulation has remained elusive. Consensus across studies from multiple species utilizing different methods to manipulate feedback is that CG feedback does not alter visual stimulus tuning or spatial properties within the classical receptive field of LGN neurons in a clear or consistent manner (Denman and

---

This article belongs to the Topical Collection: *Vision and Action*  
Guest Editors: Aasef Shaikh and Jeffrey Shall

---

Action Editor: Aasef G. Shaikh

✉ Farran Briggs  
farran\_briggs@urmc.rochester.edu

<sup>1</sup> Neuroscience Graduate Program, University of Rochester, Rochester, NY 14642, USA

<sup>2</sup> Center for Visual Science, University of Rochester, Rochester, NY 14642, USA

<sup>3</sup> Ernest J. Del Monte Institute for Neuroscience, University of Rochester School of Medicine, 601 Elmwood Ave., Box 603, Rochester, NY 14642, USA

<sup>4</sup> Center for Neural Science, New York University, New York, NY 10003, USA

<sup>5</sup> Institute for Neuroscience, University of Texas at Austin, Austin, TX 78712, USA

<sup>6</sup> Department of Psychology, University of Texas at Austin, Austin, TX 78712, USA

<sup>7</sup> Department of Neuroscience, University of Rochester School of Medicine, Rochester, NY 14642, USA

<sup>8</sup> Department of Brain and Cognitive Sciences, University of Rochester, Rochester, NY 14642, USA

Contreras 2015; Geisert et al. 1981; Gulyas et al. 1990; Hasse and Briggs 2017; Marrocco et al. 1996). Often modulations of CG feedback altered the gain of LGN neuronal responses, and in some cases these gain modulations were specific to moving stimuli or subclasses of LGN neurons (Gulyas et al. 1990; Hasse and Briggs 2017; Li et al. 2011; Marrocco et al. 1996; Przybyszewski et al. 2000; Tsumoto et al. 1978). The lack of clear CG influence on the spatial properties of LGN classical receptive fields is in fact consistent with the notion that LGN spatial properties are inherited from the retina. In contrast, compelling evidence supports alternative functional roles for CG feedback, including increasing the precision and information encoded in LGN responses to visual stimuli.

Results of studies employing non-selective methods to manipulate CG neurons suggest that CG feedback reduces response variability in LGN neurons and increases information encoded in LGN responses to visual stimuli (Andolina et al. 2007; Funke et al. 1996; McClurkin et al. 1994). McClurkin and colleagues inactivated CG neurons by reversibly cooling the occipital cortex in alert fixating monkeys. Their technical achievement was significant as was their use of alert monkeys because anesthesia may alter CG activity (Steriade 2003). These authors designed and used an extensive set of visual stimuli varying across multiple feature dimensions, and utilized an information theoretic approach to analyze the information contained in LGN spike trains in response to this rich visual stimulus set. When CG feedback was suppressed via cortical cooling, the authors observed complex effects on LGN spiking responses, including increases and decreases in spiking rates to various stimuli. Strikingly, they discovered that cortical cooling decreased stimulus-specific information in LGN neuronal spike trains and temporal distributions of spikes compared to pre-cooling responses, independent of changes in neuronal firing rates across pre-cooling and cooling conditions. Additionally, cortical cooling decreased LGN response specificity across multiple stimulus dimensions (e.g. spatial contrast, luminance, pattern). Together, the authors' findings suggested that CG feedback influenced information processing in the LGN by enhancing the separation of signals about unique stimulus features, thus improving the coding capacity of LGN neurons. In support of the notion that CG feedback enhances LGN responses to unique visual features, a more recent study employing optogenetic methods to selectively activate CG feedback demonstrated a marked increase in the precision of LGN neuronal responses to visual stimuli during CG activation (Hasse and Briggs 2017).

How might CG circuits increase response precision in the LGN? Statistically, sensory neurons behave as if their responses originate from a doubly stochastic process. Spiking activity in the LGN and in V1 is often well described as arising from a Poisson process whose rate is the product of a deterministic stimulus drive and a stochastic response gain, expressed in the “modulated Poisson model” (Goris et al.

2014). The gain summarizes slowly fluctuating modulatory influences on excitability (Goris et al. 2018). The Poisson process accounts for a baseline level of response stochasticity, which is further amplified by gain fluctuations – the larger the gain variability, the larger the response variability. This framework motivates the hypothesis that CG circuits act to stabilize the gain of LGN neurons, thereby increasing their response precision.

Guided by the work of McClurkin et al. (1994), we sought to causally test the hypothesis that CG feedback quenches response variability of LGN neurons by stabilizing their response gain, thereby increasing information coding capacity in the LGN. In the first set of experiments, we examined CG influence on LGN response variability, and in the second set of experiments, we examined CG influence on information coding among LGN neurons. In both experiments, we used virus-mediated gene delivery to optogenetically enhance the activity of CG neurons in anesthetized ferrets while recording the visual responses of LGN neurons. To assess CG influence on response variability, we analyzed LGN responses to drifting sinusoidal gratings varying in temporal frequency using the aforementioned modulated Poisson model. As hypothesized, this analysis revealed a substantial reduction in gain variability in LGN neurons with CG feedback activation. Analysis of Fano factor, a theory-agnostic measure of neuronal response dispersion, confirmed that reduced gain variability coincided with a significant reduction of overall neuronal response variance. We reasoned that the CG-mediated reduction in response variance serves to improve the sensory coding capacity of LGN neurons. In the second set of experiments, we measured changes in Fisher Information (FI) for LGN neuronal responses to gratings varying in temporal frequency and entropy rates of LGN responses to white noise m-sequence stimuli with and without activation of CG feedback. As hypothesized, causal activation of CG feedback increased FI and information rates among LGN neurons independent of changes in neuronal firing rates. Together, these findings provide strong support for the notion that CG feedback sharpens the precision of LGN responses to visual stimuli by reducing gain variability, thereby increasing stimulus-specific information coding among LGN neurons.

## 2 Materials and methods

This study involved new data collection and new analyses of data collected as a part of a previous study of the functional role of corticogeniculate (CG) circuits in vision (Hasse and Briggs 2017). Data were collected from 14 adult female ferrets (*Mustela putorius furo*) and all of the procedures performed conformed to the guidelines set forth by the NIH and the USDA and were approved by the Institutional Animal Care and Use Committees at the University of Rochester and the

Geisel School of Medicine at Dartmouth. All of the procedures involving animals have been described in detail previously (Hasse and Briggs 2017).

## 2.1 Summary of methods for which details have been published previously

All of the ferrets received an injection of a genetically modified rabies virus (SADΔG-ChR2-mCherry; titer range:  $1.3 \times 10^8$ – $4.1 \times 10^9$ ) targeting the lateral geniculate nucleus of the thalamus (LGN) in order to express channelrhodopsin2 (ChR2) and mCherry selectively in CG neurons in the visual cortex (Hasse et al. 2019; Hasse and Briggs 2017). Surgical preparation and virus injection, neurophysiological recording of LGN and V1 neurons, visual and optogenetic stimulation, spike sorting and initial data analyses, and histological processing of brain tissue have all been described in detail previously (Hasse and Briggs 2017). Briefly, in a sterile surgical procedure and under full anesthesia, 5  $\mu$ l of rabies virus was injected, targeting the LGN. Ferrets recovered for 7 to 11 days after which a terminal neurophysiological recording experiment was conducted under anesthesia and with paralytic to prevent eye movements. Multi-electrode arrays (7-channel Eckhorn Matrix from Thomas Recording GMBH, Giessen, Germany and 24-contact V-probe from Plexon Inc., Dallas, TX) placed in the LGN and in area 17 recorded LGN and V1 neurons in response to visual stimuli displayed on a CRT monitor placed ~50 cm in front of ferrets' eyes. Optogenetic activation of ChR2 was achieved with a blue LED (465 nm; Doric Lenses Inc., Quebec, CAN or Plexon, Inc., Dallas, TX) coupled to a fiber optic cable (200  $\mu$ m, NA:0.53 or 200  $\mu$ m, NA: 0.66) positioned just above the surface of area 17 near the V-probe. Light intensity at the tip of the fiber measured between 20 and 90 mW/mm<sup>2</sup>; light intensity at layer 6 is estimated to be 0.2 to 0.9 mW/mm<sup>2</sup> (Acker et al. 2016). Visual stimuli included drifting sinusoidal gratings and m-sequence white noise stimuli. Gratings were presented for 2 s with 2 s of mean gray luminance in between presentations; each grating type was displayed 2–20 times per condition (no LED, with LED). Half of the trials included visual stimulation alone (no LED) and the other half were visual stimulation paired with optogenetic activation (with LED) at the drift rate of displayed gratings or continuously on for m-sequence stimuli. Following the end of the neurophysiological recording session, ferrets were euthanized via overdose and perfused and then brain tissue was histologically processed to verify virus expression at the injection site and in CG neurons. LGN single units were spike sorted offline following standard clustering procedures. LGN neuronal tuning in response to gratings varying in contrast, temporal frequency, spatial frequency, orientation, and size, was measured via curve fits to stimulus-evoked firing rates. LGN neurons were classified as X or Y cells based on their contrast to evoke a half-

maximal response (c50 > 40% for X and < 40% for Y) and preferred temporal frequency (pref. TF < 12 Hz for X, pref. TF > 12 Hz for Y), as done previously (Derrington and Fuchs 1979; Sherman and Spear 1982). LGN neurons were classified as “intermediate” if their c50 and TF values were intermediate to those of X and Y neurons. Spatiotemporal receptive field maps for LGN and V1 neurons were generated by computing the spike-triggered average (STA) of reverse-correlated m-sequence frames.

## 2.2 Summary of animal and cell numbers

In 7 of 14 ferrets, virus was successfully injected into the LGN revealing expression of ChR2 and mCherry in CG neurons (example virus-infected and subsequently stained CG neurons in V1 shown in Fig. 1a). LGN and V1 neurons recorded in these animals are referred to as Experimental neurons throughout. In the remaining 7 ferrets, there was no virus in the LGN and no label in the visual cortex so LGN and V1 neurons recorded in these animals served as control for optogenetic activation and are referred to as Control neurons throughout. Variance and Fisher Information (FI) analyses were run on 9 Experimental LGN neurons and 8 Control LGN neurons. Entropy analyses were run on 16 Experimental LGN neurons, 14 Control LGN neurons, and an additional 6 V1 neurons (from 3 ferrets), of which 5 were Experimental and 1 was a Control neuron. Neuronal measures were qualitatively and quantitatively similar across recording sessions/animals (see Figs. 1, 2, 3 and 4) and were therefore combined into their respective categories for all population-level analyses.

## 2.3 Variability analyses

Variability analyses were performed on neuronal responses to drifting grating stimuli modulating in temporal frequency (TF). Each stimulus set consisted of 10 different temporal frequencies ranging from 1 to 32 Hz. The entire set of 10 temporal frequencies was repeated 7–20 times per neuron for each LED condition. Only LGN neurons with clear contrast tuning were used for the variability analyses to ensure that stimuli were placed within neuronal receptive fields and to confirm cell type classification. Following these criteria, 11 of 16 Experimental LGN neurons and 11 of 15 Control LGN neurons were analyzed. All LGN neurons included in the analysis also had TF tuning curves with clear preferred TFs.

For each neuron, we computed the mean and variance of the spike count for each stimulus condition. Additionally, we fit the modulated Poisson model proposed by Goris et al. (2014) to the responses of each neuron. Briefly, under this model, spikes arise from a Poisson process whose stimulus-driven rate is subject to stimulus-independent modulatory influences (gain fluctuations). If we assume that gain on average

equals 1 and fluctuates on a time-scale that is slow relative to the duration of a stimulus presentation, then response variance is given by:  $\text{var}[N|S, \Delta t] = f(S)\Delta t + \sigma_G^2(f(S)\Delta t)^2$ , where  $N$  is spike count,  $S$  is the stimulus,  $\Delta t$  is the duration of the count window,  $f(S)$  is firing rate, and  $\sigma_G$  the standard deviation of the gain. We use  $\sigma_G$  as a measure of gain variability. The first term of the right-hand side of the equation represents the Poisson process contribution to the response variance, which is equal to the mean spike count. The second term is the variance of the expected spike count conditioned on the stimulus drive, and is proportional to the square of the first term, with a proportionality factor equal to the variance of the gain signal,  $\sigma_G^2$ . To verify that the model described the data well, we performed an absolute goodness-of-fit test by comparing the log-probability of the data with the expected distribution (Goris et al. 2014). We hypothesized that activation of CG feedback would elicit a decrease in gain variability. Everything else being equal, changes in gain variability will result in changes in response variability. However, if response mean changes in conjunction with gain variability, then it is possible that either raw spike count variance or Fano factor (*i.e.*, the ratio of the spike count variance to the mean) remains constant (Henaff et al. 2020). We therefore additionally analyzed the effects of our causal manipulation on response variance and Fano factor.

For each neuron, we obtained one estimate of  $\sigma_G^2$  for each LED condition. We summarized response mean, variance, and Fano factor per neuron by averaging the corresponding estimates across all TFs. We used the Wilcoxon signed-rank test to compare these summary statistics across LED conditions within each group (Experimental or Control), and the Wilcoxon rank-sum test to compare the differences between LED conditions across groups.  $P$  values were corrected for multiple comparison at  $p < 0.0125$ . All statistical analyses are summarized in Table 1.

## 2.4 Fisher information analysis

We hypothesized that changes in gain variability brought about by activation of CG neurons would elicit changes in the coding capacity of LGN neurons. To test this hypothesis, we first estimated the FI associated with each LED condition. This statistic quantifies the amount of temporal frequency information that can be extracted from a neuronal response by an optimal decoder. Specifically, its inverse provides a lower bound on the variance of the maximum likelihood estimate. To calculate the FI, we used the following formula:

$I_F = E \left[ \frac{R'(x_{\text{ref}})^2}{\sigma(x_{\text{ref}})^2} \right]$ , where  $R'(x_{\text{ref}})$  is the derivative of the neuronal TF tuning curve computed at each TF using the “differentiate” Matlab function, and  $\sigma(x_{\text{ref}})^2$  is the variance of the spike count for that same TF (Gu et al. 2010; Nover et al. 2005; Pouget et al. 1998; Seung and Sompolinsky 1993). FI

per neuron per LED condition was quantified as the average of the FI across all TF values per condition. We used the Wilcoxon signed-rank test to compare FI across LED conditions within each group, and the Wilcoxon rank-sum test to compare the differences between LED conditions across Experimental and Control groups.

## 2.5 Entropy and information analyses

To further test whether reductions in gain variability lead to changes in visual information coding capacity of LGN neurons during causal manipulation of CG neurons, we estimated entropy and information rates from LGN and V1 responses to m-sequence stimuli following the methods of Strong et al. (1998). Procedures for computing entropy from m-sequence responses were modeled after those described by Liu et al. (2001). Only neurons with well-defined spatial receptive fields with widths on the order of a single m-sequence grid pixel (grid pixel range: 0.9375 to 2.5 degrees, average grid pixel:  $1.65 \pm 0.1$  degrees) were used for these analyses (ON and OFF spatial receptive fields for two example neurons illustrated in Fig. 1b). All analyses were performed for two conditions per neuron: with and without LED applied to the surface of V1. Both conditions were analyzed for Experimental and Control neurons and differences in entropy and information across LED conditions were then compared between Experimental and Control LGN neurons.

Separate sets of neuronal spiking responses to m-sequence stimulation were utilized to compute response and noise entropy. For response entropy, neuronal spiking responses over the entire m-sequence presentation were analyzed. For noise entropy, responses to 6 consecutive frames (20 ms per frame) of the preferred luminance increment or decrement (three frames of white then three frames of black or *vice versa*) in the pixel covering the classical receptive field were used (similar to the approach by Liu et al. 2001). There were ~ 500 repeats of this frame sequence per m-sequence presentation for which repeated neuronal responses were measured to compute noise entropy.

Neuronal spike times, sampled at 40KHz, were discretized into “letters” with bin width ( $\Delta\tau$ ) = 8 ms. If at least 1 spike occurred in a bin, the letter was assigned a value of 1, otherwise it was 0. Different bin widths (4, 6, and 8 ms) were tested and response entropy scaled with increasing bin width. Furthermore, no neurons had greater than 5% of bins with more than 1 spike using a bin width of 8 ms, so this bin width was used for all subsequent steps. By altering the number of bins per word ( $W$ ), the word length ( $T$ ) was varied according to:  $T = W\Delta\tau$ . Multiple sizes for  $T$  were tested between 16 and 96 (*i.e.*  $W$  varying from 2 to 16) to provide consistent estimates of true entropy after correction for finite data (Strong et al. 1998), described below. Each naïve entropy

rate, listed below, was computed using the same general equation for naïve entropy rate  $= -\sum_i p_i \log_2 p_i / T$ , where  $p_i$  is the probability of occurrence of the  $i^{\text{th}}$  word. Response entropy rate was computed from the words generated from the neuronal spiking response to the ongoing m-sequence. Noise entropy rate was computed from the words generated in response to each 6-frame preferred luminance modulation sequence and then averaged over all repeats of this sequence (Liu et al. 2001). Maximum entropy rate was computed from the probability distribution of all possible words given the mean firing rate (Pryluk et al. 2019). To correct for finite data, the following extrapolation procedure was performed for each fixed size  $T$ . The m-sequence data were partitioned as the full m-sequence presentation, two halves, three thirds, and four quarters of the m-sequence presentation. Naïve maximum and response entropy rates were computed per partition; for halves, thirds, and quarters of the data, values from each segment were averaged. Naïve information rate was also computed per partition as response entropy rate minus the average of noise entropy rates over all preferred luminance modulation sequences in the partition; values for each segment were averaged as above. These naïve entropy rates were then plotted against the inverse fraction of data used and the true entropy rate was computed by finding the y-intercept of a regression line fit to the naïve entropy rate estimates. This procedure was repeated for different sizes of  $T$  and true entropy rates were plotted against inverse  $T$  to ensure that true entropy rates were reliable for a range of  $T$  sizes, taking into account biases associated with larger  $T$  and finite data size. Finally, true information rate values per neuron were divided by the average spike rate across the entire m-sequence presentation to obtain information in bits/spike. As mentioned above, all of these steps were performed separately for m-sequence presentations with and without LED activation of CG feedback for each neuron.

Maximum entropy rate, response entropy rate, information rate, and information in bits/spike were displayed separately for X, Y, and intermediate LGN cell types, however because there were only a few classified neurons per Experimental and Control group, statistical comparisons were made across all LGN neurons. Within group comparisons of entropy rates and information were made using Wilcoxon signed-rank tests. Differences in entropy rates and information (with LED – no LED values) across Experimental and Control LGN groups were tested using Wilcoxon rank-sum tests with  $p$  value correction for multiple comparisons ( $p < 0.025$ ). Only average data are reported for V1 neurons because there was only 1 Control V1 neuron. All statistics from entropy and information analyses are reported in Table 2. Although firing rates were slightly higher among LGN and V1 Experimental neurons with LED activation, firing rates were not significantly

different across LED conditions for any of the neuronal groupings ( $p > 0.2$  for all; average  $\pm$  SEM firing rate for: Experimental LGN no LED =  $6.7 \pm 0.7$ , LED =  $7.0 \pm 0.8$ ; Control LGN no LED =  $12.6 \pm 3.4$ , LED =  $12.9 \pm 3.4$ ; Experimental V1 no LED =  $9.7 \pm 3.8$ , LED =  $10.0 \pm 2.9$ ).

### 3 Results

Based on previous evidence that CG feedback modulates the variability of LGN activity in response to visual stimuli (Andolina et al. 2007; Funke et al. 1996), increases the spike timing precision of LGN responses (Hasse and Briggs 2017), and enhances the information coding capacity of LGN neurons (McClurkin et al. 1994), we tested the hypothesis that CG feedback enhances information coding among LGN neurons by stabilizing the response gain of LGN neurons. We utilized modern selective optogenetic methods to characterize the causal influence of CG neurons on gain variability and information coding capacity of LGN neurons.

To determine the effects of CG feedback on trial-to-trial fluctuations in neuronal response gain, we analyzed LGN neuronal responses across 7–20 repeats of a series of drifting gratings varying in temporal frequency (TF), both with and without optogenetic activation of CG feedback. We described neuronal activity with a statistical model designed to identify the contribution of gain fluctuations to overall response variability: the modulated Poisson model (Goris et al. 2014). We performed this analysis on 9 Experimental LGN neurons from 2 ferrets in which virus-infected CG neurons expressed ChR2 (Fig. 1a) and on 8 Control LGN neurons from 1 ferret in which ChR2 was not expressed in CG neurons. All LGN neurons tested displayed tuning for contrast as well as TF (Fig. 1c, d), which enabled classification of LGN neurons as X, Y, or intermediate based on their c50 and preferred TF. In the vast majority of cases (31 out of 34), the modulated Poisson model accurately captured the structure of the measured response distributions, *i.e.* the model description could not be distinguished from the real data. For each LGN neuron, we used this model to obtain an estimate of gain variability for both LED conditions (examples illustrated in Fig. 1c, d).

There was a 4-fold reduction in gain variability across LED conditions for Experimental LGN neurons (from  $0.25 \pm 0.085$  to  $0.049 \pm 0.025$ ; Fig. 2a). In contrast, there was no change in gain variability for Control LGN neurons ( $0.19 \pm 0.083$  to  $0.15 \pm 0.064$ ; Fig. 2a). Changes in gain variability can, but need not, result in changes in overall response variance, as variance also depends on changes in the mean response level. We found that optogenetic activation of CG feedback did not yield a systematic change in response strength: mean spike counts did not differ across LED conditions for Experimental or Control LGN neurons (Fig. 2b; Table 1). As a consequence, all but one Experimental LGN neuron

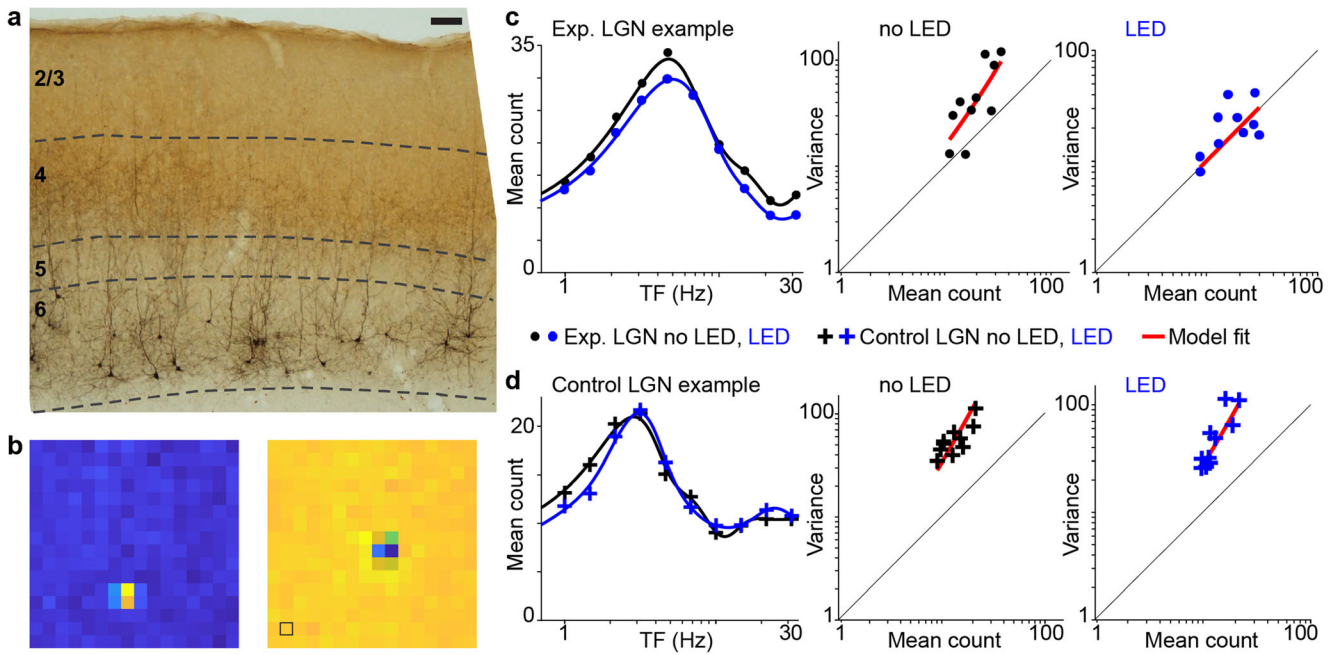


**Fig. 1** Example virus-infected CG neurons, LGN neuronal spatial receptive field maps, and temporal frequency responses. **a.** Coronal section through V1 (area 17) stained against cytochrome oxidase activity with virus-infected CG neurons visible following antibody and DAB-peroxide staining. Layers are indicated with dashed gray lines and labeled at left. Scale bar represents 100  $\mu$ m. **b.** Representative spatial receptive field maps for ON center (left) and OFF center (right) LGN neurons. Black box width corresponds to 1 degree and applies to both spatial receptive

field maps. Note that the centers of each receptive field are mostly captured by single bright/dark pixels. **c.** Temporal frequency (TF) tuning curves (left) and variance to mean comparisons without (black, middle) and with (blue, right) LED illumination of V1 for a representative Experimental LGN neuron (data illustrated with filled circles). Fit of the modulated Poisson model (Goris et al. 2014) to the data is shown in red. **d.** Same as **c** but showing a representative Control LGN neuron (data illustrated with crosses)

displayed a decrease in spike count variance with LED activation of CG feedback (Fig. 2c). This effect was significant within the Experimental LGN neuronal group ( $p = 0.0078$ ; Table 1). Additionally, the reduction in spike count variance with LED activation of CG feedback was significantly greater in Experimental compared to Control LGN neurons ( $p = 0.0108$ ; Fig. 2c; Table 1). Neuronal response variability is

often quantified with Fano factor, a normalized measure of response dispersion. Consistent with the trends described above, LED activation of CG neurons significantly reduced Fano factor for Experimental LGN neurons ( $p = 0.0078$ ), but not for Control LGN neurons (Fig. 2d; Table 1).

To determine whether a reduction in response variance could serve to improve the sensory coding capacity of LGN

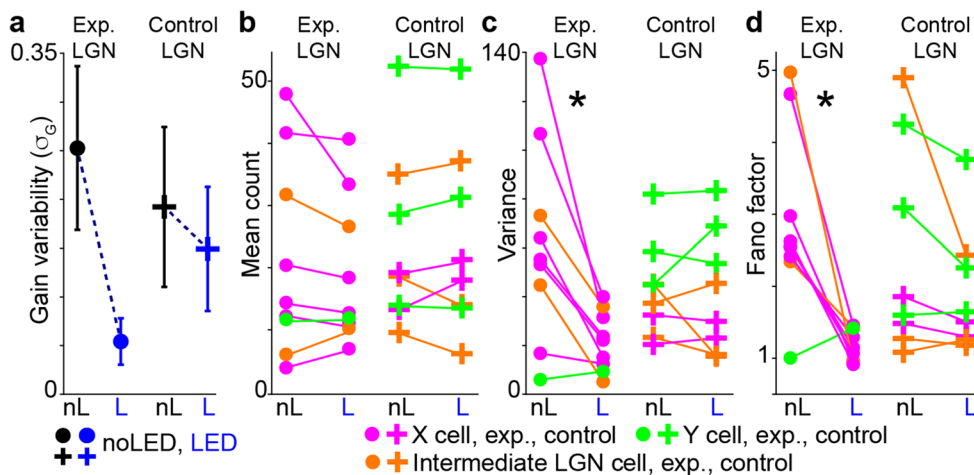


**Fig. 2** Variance in LGN responses with and without optogenetic activation of CG neurons. Changes in gain variability (**a**), mean spike count (**b**), variance in spike count (**c**), and Fano factor (**d**), across no LED (nL) and LED (L) trials for Experimental (filled circles) and

Control (crosses) LGN neurons. LGN cell classifications are indicated in the keys at the bottom. Asterisks indicate significant differences within a group across LED conditions. Average values and statistics listed in Table 1

**Table 1** Variance analysis statistics

		$\sigma_G$	Mean Spike Count	Variance	Fano Factor	Fisher Information
Experimental LGN <i>n</i> = 9 cells <i>n</i> = 2 ferrets	Mean $\pm$ SEM No LED	0.25 $\pm$ 0.085	21.03 $\pm$ 5.27	61.95 $\pm$ 13.66	2.90 $\pm$ 0.40	2.18 $\pm$ 2.01
	Mean $\pm$ SEM LED	0.049 $\pm$ 0.025	18.88 $\pm$ 3.97	21.72 $\pm$ 4.070	1.18 $\pm$ 0.074	2.70 $\pm$ 2.17
	P value in group	0.109	0.359	<b>0.0078</b>	<b>0.0078</b>	<b>0.0078</b>
	Mean $\pm$ SEM difference (LED-No LED)	-0.23 $\pm$ 0.10	-2.14 $\pm$ 1.77	-40.23 $\pm$ 10.83	-1.72 $\pm$ 0.43	0.37 $\pm$ 0.12
Control LGN <i>n</i> = 8 cells <i>n</i> = 1 ferret	Mean $\pm$ SEM No LED	0.19 $\pm$ 0.083	23.78 $\pm$ 5.06	43.01 $\pm$ 7.08	2.44 $\pm$ 0.52	0.18 $\pm$ 0.076
	Mean $\pm$ SEM LED	0.15 $\pm$ 0.064	24.01 $\pm$ 5.31	42.03 $\pm$ 25.21	1.92 $\pm$ 0.31	0.20 $\pm$ 0.092
	P value in group	0.0391	0.844	0.844	0.0547	1
	Mean $\pm$ SEM difference (LED-No LED)	-0.0431 $\pm$ 0.02	0.228 $\pm$ 1.10	-2.90 $\pm$ 7.03	-0.736 $\pm$ 0.36	0.022 $\pm$ 0.047
Experimental vs Control	P value differences	0.229	0.3619	<b>0.0108</b>	0.0386	<b>0.0045</b>

Average  $\pm$  SEM gain variability ( $\sigma_G$ ), mean spike count, spike count variance, and Fano factor for Experimental (top box) and Control (second box) LGN neurons including statistical comparisons. Average  $\pm$  SEM mean spike count, variance in spike count, and Fano factor are averaged for each neuron across all grating presentations. Wilcoxon rank tests were used for within-group comparisons and for Experimental *versus* Control difference measures with *p* values corrected for multiple comparisons (*p* < 0.0125; bold text)

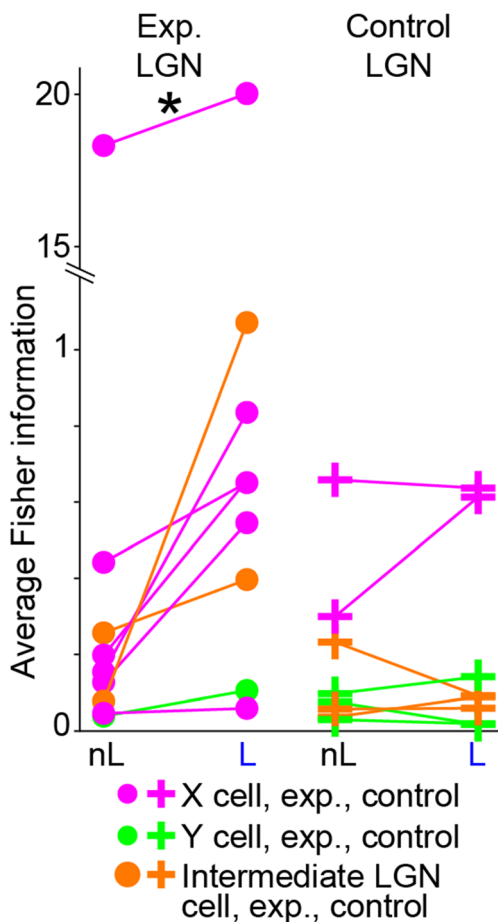


**Fig. 3** Fisher information in LGN responses with and without optogenetic activation of CG neurons. Fisher information (FI) computed from the same TF tuning data for Experimental LGN neurons (left, filled circles) and Control LGN neurons (right, crosses) used in the variance analyses. Average FI is shown for each neuron across no LED (nL) and LED (L) conditions. LGN cell classifications are indicated in the key at the bottom. Asterisk indicates a significant difference within the Experimental LGN group across LED conditions

neurons, we first examined FI for each neuron with and without of LED activation of CG feedback (Gu et al. 2010; Nover et al. 2005). This statistic quantifies the amount of temporal frequency information that can be extracted from a neuronal response by an optimal decoder. In keeping with our hypothesis, we observed a significant increase in FI among Experimental LGN neurons with LED activation of CG feedback (*p* = 0.0078; Fig. 3, left; Table 1), but no change across LED conditions for Control LGN neurons (*p* = 1; Fig. 3, right; Table 1). Correspondingly, the difference across LED conditions for Experimental LGN neurons was significantly greater than the difference across LED conditions for Control LGN neurons (*p* = 0.0045; Table 1).

To further test whether CG-mediated reductions in response variance alter the visual information coding capacity of LGN neurons, we examined entropy rates for LGN responses to white noise m-sequence stimuli during selective causal manipulation of CG neurons. We also explored whether LED activation of CG neurons within V1 altered information coding among V1 neurons. LGN and V1 neurons with well-defined spatiotemporal receptive field maps generated from m-sequence stimulation were utilized for this analysis and the vast majority of LGN and V1 neurons tested had classical receptive fields that were mostly encompassed by a single pixel of the m-sequence grid (e.g. Figure 1b; average grid pixel = 1.65  $\pm$  0.1 degrees). LGN and V1 neurons tested also were tuned for contrast and temporal frequency, which enabled classification of LGN neurons as X, Y, or intermediate based on their c50 and preferred TF. A total of 16 Experimental LGN neurons, 14 Control LGN neurons, 5 Experimental V1 neurons, and 1 Control V1 neuron were analyzed (Table 2).

We first assessed the extent to which LGN and V1 neuronal responses to m-sequence stimulation approached maximum entropy estimates (Pryluk et al. 2019). Comparison of

**Table 2** Entropy analysis statistics

		Max entropy	Response entropy	Info. (bits/s)	Info. (bits/spike)
Experimental LGN <i>n</i> = 16 cells <i>n</i> = 5 ferrets	Mean ± SEM No LED	35.5 ± 2.8	37.1 ± 2.6	23.9 ± 1.5	3.89 ± 0.3
	Mean ± SEM LED	42.1 ± 3.6	43.4 ± 3.3	27.7 ± 2.0	4.32 ± 0.3
	P value in group	0.0734	0.0523	0.0523	0.0676
	Mean ± SEM difference (LED-No LED)	6.7 ± 2.0	6.3 ± 1.9	3.9 ± 1.2	0.43 ± 0.1
Control LGN <i>n</i> = 14 cells <i>n</i> = 6 ferrets	Mean ± SEM No LED	50.4 ± 7.2	50.5 ± 6.9	32.5 ± 5.2	3.2 ± 0.2
	Mean ± SEM LED	49.6 ± 6.8	49.7 ± 6.3	31.7 ± 4.8	3.1 ± 0.3
	P value in group	0.9999	0.9451	0.9999	0.4213
	Mean ± SEM difference (LED-No LED)	−0.87 ± 2.2	−0.85 ± 2.3	−0.83 ± 1.6	−0.09 ± 0.1
Experimental <i>vs</i> Control	P value differences	<b>0.0119</b>	<b>0.0150</b>	<b>0.0210</b>	<b>5.18 × 10<sup>−4</sup></b>
Experimental V1 <i>n</i> = 5 cells <i>n</i> = 2 ferrets	Mean ± SEM No LED	43.7 ± 12.4	43.5 ± 12.2	28.3 ± 8.7	3.4 ± 0.4
	Mean ± SEM LED	49.5 ± 11.1	48.9 ± 10.6	32.5 ± 7.0	3.8 ± 0.5
	Mean ± SEM difference (LED-No LED)	5.8 ± 5.1	5.4 ± 5.6	4.2 ± 5.7	0.33 ± 0.2
	Control V1 <i>n</i> = 1 cell <i>n</i> = 1 ferrets	Mean ± SEM No LED	23.8	25.8	23.9
	Mean ± SEM LED	38.6	39.0	24.4	3.6
	Mean ± SEM difference (LED-No LED)	14.8	13.2	0.47	−1.88

Average ± SEM maximum entropy rate (bits/s), response entropy rate (bits/s), information rate (bits/s), and information (bits/spike) for Experimental LGN (top box), Control LGN (second box), Experimental V1 (third box), and Control V1 (fourth box) neurons including statistical comparisons. Wilcoxon rank tests were used for within-group comparisons and for Experimental *versus* Control difference measures with *p* values corrected for multiple comparisons for entropy and information comparisons ( $p < 0.025$ ; bold text)

maximum entropy and response entropy revealed that LGN neurons in both Experimental and Control groups had response entropy measures that approached maximum entropy estimates (Fig. 4a). Maximum and response entropy estimates were larger with LED activation of CG feedback for Experimental LGN neurons (Fig. 4a, left, compare blue *versus* black symbols, and Fig. 4c, leftmost; Table 2), although these differences were not statistically significant within the Experimental LGN neuronal group. However, the differences in maximum and response entropy estimates across LED conditions were significantly larger for Experimental compared to Control LGN neurons ( $p < 0.015$  for both, Table 2; Fig. 4a, c). Interestingly, both maximum and response entropy estimates also tended to be larger with LED activation of CG neurons for Experimental V1 neurons, although there were not enough Control V1 neurons for a statistical comparison (Table 2). It is possible that response entropy scaled with increases in neuronal firing rate, which dictates the maximum entropy estimate. However, although neuronal firing rates were slightly higher with LED activation for Experimental LGN and V1 neurons, firing rates were not significantly different across LED conditions for any neuronal group ( $p > 0.2$  for all).

To explore whether increases in entropy estimates with LED activation of CG neurons were due to subtle increases

in neuronal firing rate or increases in information coding capacity, we measured information coding capacity without and with LED activation of CG feedback. Because LED activation of CG neurons caused an increase in response entropy among Experimental neurons, an increase in information rate would require no change or a decrease in response variability, quantified as noise entropy. We hypothesized that LED activation of CG feedback would reduce variability in responses to repeated stimulus presentations, as shown above, thus reducing noise entropy and increasing information rates among LGN Experimental neurons. For all but two Experimental LGN neurons, LED activation of CG feedback led to an increase in information rate (Fig. 4b, left and Fig. 4d; filled circles). In contrast, information rates among Control LGN neurons were similar across LED conditions (Fig. 4b, left and Fig. 4d; crosses). Furthermore, the increase in information rate with LED activation of CG feedback was significantly larger for Experimental LGN neurons compared to Control LGN neurons ( $p = 0.0210$ ; Table 2). Importantly, the significant increase in information rate with LED activation of CG feedback among Experimental LGN neurons was not simply due to changes in neuronal firing rate because when information rate was normalized by neuronal firing rate to generate information in bits/spike, all but one Experiment LGN neuron

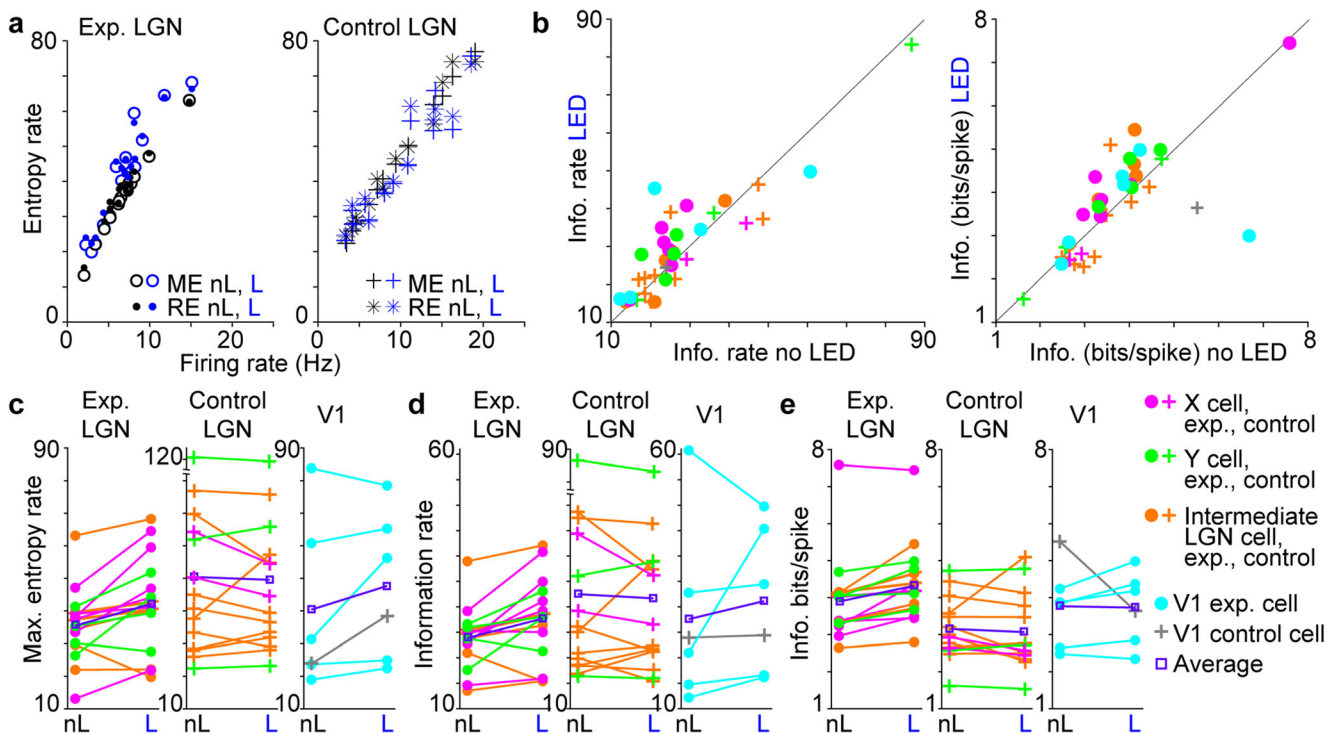


**Fig. 4** Entropy and information in LGN responses with and without optogenetic activation of CG neurons. **a.** Relationships between maximum entropy (ME; open circles & crosses) or response entropy (RE; filled circles & asterisks) rate in bits/s and firing rate for Experimental (left) and Control (right) LGN neurons. Black symbols are responses on no LED (nL) trials and blue are responses on LED (L) trials. **b.** Information rate (bits/s) at left and information in bits/spike at right across LED conditions for LGN and V1 Experimental and Control neurons. Color and symbol key below. Note that Experimental LGN

neurons (filled magenta, green, and orange circles) are mostly above the diagonals representing unity. Changes in maximum entropy rate in bits/s (**c**), information rate in bits/s (**d**), and information in bits/spike (**e**) across no LED (nL) and LED (L) trials for individual Experimental LGN (left, filled circles), Control LGN (middle, crosses), and V1 (right, cyan filled circles = Experimental, gray crosses = Control) neurons. LGN cell classifications are indicated in the key at far right; average data illustrated in purple. Average values and statistics listed in Table 2

demonstrated an increase in information (bits/spike) with LED activation of CG feedback (Fig. 4b, right and Fig. 4e; filled circles). In contrast, information coding did not change across LED conditions for Control LGN neurons (Fig. 4b, right and Fig. 4e; crosses). Again, the increase in information in bits/spike with LED activation of CG feedback was significantly larger for Experimental LGN neurons compared to Control LGN neurons ( $p = 5.18 \times 10^{-4}$ ; Table 2). Most Experimental V1 neurons also demonstrated an increase in information rate and information (bits/spike) with LED activation of CG neurons (Fig. 4b-e, cyan filled circles; Table 2), although there were not enough samples for statistical comparisons within or across Experimental and Control V1 neuronal groupings.

### 4 Discussion

Our objective in this study was to determine whether CG circuits serve to stabilize the response gain of LGN neurons, thereby enhancing their information coding capacity. Optogenetic activation of CG feedback did not alter LGN

neuronal tuning for temporal frequency, nor did it modulate LGN neuronal firing rates in a systematic manner (Figs. 1c, d and 2b), consistent with previous findings (Denman and Contreras 2015; Hasse and Briggs 2017; Marrocco et al. 1996). However, activation of CG feedback reduced gain variability (Fig. 2a), which in turn reduced response variability (Fig. 2c-d), and increased coding capacity for temporal frequency (Fig. 3). We further explored whether selective and causal manipulation of CG feedback altered information rates among LGN neurons. Optogenetic activation of CG feedback increased information rates for the vast majority of Experimental LGN neurons (Fig. 4b-e), an effect that was absent for Control LGN neurons (Fig. 4). Together these results suggest that the role of CG feedback is to increase the precision of visual stimulus information encoding in the LGN through reduction in the variability of LGN responses to relevant visual stimulus features. This facilitating effect is reminiscent of facilitation attributed to top-down attention mechanisms in the visual cortex (Rabinowitz et al. 2015).

Prior studies of LGN neuronal response variability have produced differing estimates of Fano factor. While some

reported sub-Poisson variability in the range of  $\sim 0.3$  (Kara et al. 2000) to  $\sim 0.55$  (Kumbhani et al. 2007), others reported wider ranging sub- to super-Poisson variability dependent upon stimulus type, cell types, and size of the calculation window (Hartveit and Heggelund 1994; Levine et al. 1996; Andolina et al. 2007; Liu et al. 2001). We observed Fano factors that were consistently above Poisson, but were in a similar range as those reported previously (Andolina et al. 2007; Goris et al. 2014). Importantly, Fano factors in our dataset were similar across LGN neurons recorded from both Experimental and Control animals (Table 1). There are two possible explanations for why we observed larger Fano factors compared to some prior studies. First, we computed Fano factor from responses to drifting gratings varying in temporal frequency while prior studies reporting lower Fano factors used stationary gratings or gratings varying in contrast but optimized for other parameters (Kara et al. 2000; Kumbhani et al. 2007). Second, we averaged Fano factors across a range of TFs including non-preferred TFs, for all neurons. Rather than limiting our analysis to preferred TFs, inclusion of all stimulus conditions may have produced higher Fano factors compared to results obtained using more optimized stimulus conditions. Inclusion of responses to all presented TFs was purposeful to facilitate better estimation of gain variability using the modulated Poisson model.

Our sample of LGN neurons from which we measured response variability did not include sufficient Y cells to make conclusions about differences in response variability across cell classes. The majority of our Experimental LGN neurons were X cells or LGN neurons with intermediate tuning. Our single Experimental Y cell showed very low variance in the no LED condition, making it challenging to assess further reductions in variability. Although some prior studies did not report cell type or did not observe differences in variability across LGN cell types (Andolina et al. 2007; Liu et al. 2001), evidence from a handful of other studies suggest there may be cell type specific differences in response variability. In these reports, Y cells demonstrated higher response reliability and precision and lower Fano factors compared to X cells (Hartveit and Heggelund 1994; Levine et al. 1996; Kumbhani et al. 2007). Interestingly, when we measured the effects of optogenetic activation of CG feedback on LGN response timing and precision, we observed similar reductions in response latency and increases in response precision across X and Y cells (Hasse and Briggs 2017). It is possible that differences in X and Y neuronal response variability are due to biases in responses to certain visual stimuli and that unique stimuli optimized to each cell type generate similar response variability. Alternatively, X and Y neurons could encode visual information differently, explored further below, leading to differential variability estimates. It is noteworthy though that optogenetic activation of CG feedback increases response precision in both X and Y LGN neurons, suggesting that

whatever the baseline rate of variability, CG feedback serves to improve response precision.

Reassuringly, the information values in rate and bits/spike we observed were within the range of those reported previously for LGN neurons recorded in anesthetized cats (Kumbhani et al. 2007; Liu et al. 2001; Rathbun et al. 2010; Reinagel and Reid 2000). Comparison to the values reported by McClurkin and colleagues is not straightforward as they reported transmitted information in bits. Instead of using spike trains or spike histograms, McClurkin and colleagues used spike density functions or temporal components of spiking responses to stimuli and reported transmitted information as the difference between responses to all stimuli and responses to shuffled stimuli. They also normalized by information in control conditions, causing transmitted information values to be close to zero (McClurkin et al. 1991; McClurkin et al. 1994). It is also important to reiterate that McClurkin and colleagues studied information coding in the LGN of alert and fixating monkeys, so there could be differences in information coding capacity across carnivores and primates and/or due to arousal state. Interestingly, McClurkin et al. (1994) did not observe robust changes in LGN response variance across cortical cooling conditions, an effect they attributed to their use of alert fixating monkeys. Taking into consideration important differences in method, species, wakefulness, and information calculations, it is nonetheless noteworthy that McClurkin et al. (1994) observed a roughly 25% reduction in transmitted information among LGN neurons when the cortex was cooled while we observed a 12% increase in information in bits/spike when CG feedback is enhanced.

We observed similar increases in information rate and information in bits/spike across X, Y, and intermediately classified Experimental LGN neurons. We also observed roughly similar increases in information coding for Experimental V1 neurons, most of which were located on deeper contacts and were presumably Simple cells in layer 6 of V1 given their linear receptive fields. Most prior studies of information coding in LGN neurons reported small samples dominated by one LGN cell type, or cell type was not reported (Liu et al. 2001; Rathbun et al. 2010; Reinagel and Reid 2000). However, one study with a substantial dataset reported significant differences in bits/spike for X and Y LGN neurons (Kumbhani et al. 2007). In the Kumbhani et al. (2007) study, these authors observed greater information in bits/spike for Y cells compared to X cells, which they attributed to the fact that X cells encoded more information in temporal patterns compared to Y cells. This latter notion is consistent with the results reported by McClurkin et al. (1994) in which they recorded predominantly from parvocellular LGN neurons and noted significant reductions in transmitted information assessed both with LGN neuronal spike

density functions and temporal components. A likely explanation for why we did not observe differences in information coding across LGN cell types is that we used white noise stimuli rather than gratings (Kumbhani et al. 2007) or patterns (McClurkin et al. 1994). While grating and patterned stimuli are likely to drive X and Y (or parvocellular and magnocellular) LGN neurons differently, white noise stimuli may elicit more similar responses due to the lack of correlation structure and rapid temporal dynamics.

Although entropy-based estimates of information and FI are entirely distinct measurements, at the core of each are estimates of neuronal response variability. Here we demonstrate that optogenetic activation of CG feedback caused dramatic reductions in response variability and corresponding increases in information assessed independently using two distinct measurements. Critically, changes in variability and information following activation of CG feedback were independent of changes in neuronal firing rate or tuning. Additionally, reductions in variability and increases in information coding were only present in Experimental LGN neurons recorded in animals in which virus injected into the LGN drove expression of Chr2 in CG neurons; LGN neurons recorded in Control animals never showed changes across LED conditions. Although all of these recordings were made in anesthetized animals, it is remarkable that reductions in LGN response variability caused by optogenetic activation of CG feedback resembled attention-mediated reductions in response variability observed in V4 of behaving monkeys (Rabinowitz et al. 2015). Attention focused upon a visual stimulus increases observers' ability to perceive small changes in stimulus attributes (Carrasco et al. 2004). This behavioral effect is associated with mild increases in mean neuronal response rates among visual cortical neurons (Maunsell and Cook 2002) and comparatively stronger reductions in neuronal response variability (Cohen and Maunsell 2009; Mitchell et al. 2009). Attention specifically reduces the component of neuronal response variability that stems from trial-to-trial fluctuations of modulatory signals (Rabinowitz et al. 2015). Interestingly, the effect of attention on response variability is strikingly similar to the effect of optogenetic activation of CG feedback on LGN response variability described here. Accordingly, CG circuits may serve to stabilize the response gain of LGN neurons in order to relay attention signals and to enhance the encoding of task-relevant stimulus feature information. fMRI and single-neuron neurophysiological experiments have demonstrated attentional modulation of LGN activity (Ling et al. 2015; McAlonan et al. 2008; O'Connor et al. 2002; Vanduffel et al. 2000), and attention enhances communication between neurons in the deepest layers of V1 and the LGN

(Mock et al. 2018). Together these results suggest that CG feedback could convey a combination of visual and cognitive signals to the LGN via a unifying mechanism of response variability quenching.

Although information coding among LGN neurons has been studied extensively (Kumbhani et al. 2007; Liu et al. 2001; McClurkin et al. 1991; McClurkin et al. 1994; Rathbun et al. 2010; Reinagel and Reid 2000), only recently have methods for selective and reversible manipulation of CG neurons become available. Inspired by the findings of McClurkin and colleagues, we used selective CG manipulation to causally test the precise contribution of CG feedback to LGN information coding. Our guiding hypothesis was that increased information coding capacity among LGN neurons is generated through quenching of response variability. Analyses of responses to a variety of visual stimuli revealed systematic reductions in response variability and increases in information coding capacity. Together these findings paint a more detailed picture of the role of CG feedback in enhancing the precision and reliability of LGN responses through reduced variability. More broadly, comparison of optogenetic data in anesthetized animals to data obtained from alert and attending animals suggests that top-down feedback circuits could utilize similar variability quenching mechanisms to enhance relevant visual feature encoding.

**Acknowledgements** We thank Brianna Carr, Marc Mancarella, and Elise Bragg for expert technical assistance and Drs. Dana LeMoine, Wendy Bates, Diane Moorman-White, Jeff Wyatt, Karen Moodie, and Kirk Maurer for veterinary assistance. We thank Dr. Daniel Rathbun, Uday Chockanathan, and Dr. Krishnan Padmanabhan for helpful discussions of data analysis methods and comments on this manuscript.

**Author contributions** A.J.M., R.L.T.G., and F.B. designed the experiments. A.J.M. and J.M.H. collected the data. A.J.M., L.S., and F.B. analyzed the data. A.J.M., R.L.T.G., and F.B. wrote the manuscript.

**Funding information** This work was funded by the National Institutes of Health (National Eye Institute: EY018683 and EY025219 to F.B. and T32EY007125 to A.J.M.) and the Whitehall Foundation (2013-05-06). J.M.H. was supported by a Graduate Fellowship from the Albert J. Ryan Foundation.

## Compliance with ethical standards

**Conflicts of interest/competing interests** All of the authors declare no financial conflicts of interest or competing interests related to this study.

**Availability of data and material** Data generated for this study will be made available upon reasonable written request to the corresponding author.

**Code availability** Variance code is available here: <https://gorislab.github.io/resources/> Information theory analysis code is available here: <https://github.com/BriggsNeuro/InfoVarianceCode>.

## References

- Acker, L., Pino, E. N., & Desimone, R. (2016). FEF inactivation with improved optogenetic methods. *Proceedings of the National Academy of Science USA*, *113*, E7297–E7306.
- Andolina, I. M., Jones, H. E., Wang, W., & Sillito, A. M. (2007). Corticothalamic feedback enhances stimulus response precision in the visual system. *PNAS*, *104*(5), 1685–1690.
- Carrasco, M., Ling, S., & Read, S. (2004). Attention alters appearance. *Nature Neuroscience*, *7*(3), 308–313.
- Cohen, M. R., & Maunsell, J. H. (2009). Attention improves performance primarily by reducing interneuronal correlations. *Nature Neuroscience*, *12*(12), 1594–1600.
- Denman, D. J., & Contreras, D. (2015). Complex effects on in vivo visual responses by specific projections from mouse cortical layer 6 to dorsal lateral geniculate nucleus. *Journal of Neuroscience*, *35*(25), 9265–9280.
- Derrington, A. M., & Fuchs, A. F. (1979). Spatial and temporal properties of X and Y cells in the cat lateral geniculate nucleus. *Journal of Physiology*, *293*, 347–364.
- Erisir, A., Van Horn, S. C., Bickford, M. E., & Sherman, S. M. (1997a). Immunocytochemistry and distribution of parabrachial terminals in the lateral geniculate nucleus of the cat: A comparison with corticogeniculate terminals. *The Journal of Comparative Neurology*, *377*, 535–549.
- Erisir, A., Van Horn, S. C., & Sherman, S. M. (1997b). Relative numbers of cortical and brainstem inputs to the lateral geniculate nucleus. *PNAS*, *94*, 1517–1520.
- Funke, K., Nelle, E., Li, B., & Worgotter, F. (1996). Corticofugal feedback improves the timing of retino-geniculate signal transmission. *NeuroReports*, *7*(13), 2130–2134.
- Geisert, E. E., Langsetmo, A., & Spear, P. D. (1981). Influence of the cortico-geniculate pathway on response properties of cat lateral geniculate nucleus. *Brain Research*, *208*, 409–415.
- Goris, R. L. T., Movshon, J. A., & Simoncelli, E. P. (2014). Partitioning neuronal variability. *Nature Neuroscience*, *17*(6), 858–865.
- Goris, R. L. T., Ziemba, C. M., Movshon, J. A., & Simoncelli, E. P. (2018). Slow gain fluctuations limit benefits of temporal integration in visual cortex. *Journal of Vision*, *18*(8), 1–13.
- Gu, Y., Fetsch, C. R., Adeyemo, B., DeAngelis, G. C., & Angelaki, D. E. (2010). Decoding of MSTd population activity accounts for variations in the precision of heading perception. *Neuron*, *66*, 596–609.
- Gulyas, B., Lagae, L., Eysel, U. T., & Orban, G. A. (1990). Corticofugal feedback influences the responses of geniculate neurons to moving stimuli. *Experimental Brain Research*, *79*(2), 441–446.
- Hartveit, E., & Heggelund, P. (1994). Response variability of single cells in the dorsal lateral geniculate nucleus of the cat. Comparison with retinal input and effect of brain stem stimulation. *Journal of Neurophysiology*, *72*, 1278–1289.
- Hasse, J. M., Bragg, E. M., Murphy, A. J., & Briggs, F. (2019). Morphological heterogeneity among corticogeniculate neurons in ferrets: Quantification and comparison with a previous report in macaque monkeys. *Journal of Comparative Neurology*, *527*, 546–557.
- Hasse, J. M., & Briggs, F. (2017). Corticogeniculate feedback sharpens the temporal precision and spatial resolution of visual signals in the ferret. *Proceedings of the National Academy of Science USA*, *114*(30), E6222–E6230.
- Henaff, O. J., Boundy-Singer, Z. M., Meding, K., Ziemba, C. M., & Goris, R. L. T. (2020). Representation of visual uncertainty through neural gain variability. *Nature Communications*, *11*(2513), 1–12.
- Kara, P., Reinagel, P., & Reid, R. C. (2000). Low response variability in simultaneously recorded retinal, thalamic, and cortical neurons. *Neuron*, *27*, 635–646.
- Kumbhani, R. D., Nolt, M. J., & Palmer, L. A. (2007). Precision, reliability, and information-theoretic analysis of visual thalamocortical neurons. *Journal of Neurophysiology*, *98*, 2647–2663.
- Levine, M. W., Cleland, B. G., Mukherjee, P., & Kaplan, E. (1996). Tailoring of variability in the lateral geniculate nucleus of the cat. *Biological Cybernetics*, *75*, 219–227.
- Li, G., Ye, X., Song, T., Yang, Y., & Zhou, Y. (2011). Contrast adaptation in cat lateral geniculate nucleus and influence of corticothalamic feedback. *European Journal of Neuroscience*, *34*, 622–631.
- Ling, S., Pratte, M., & Tong, F. (2015). Attention alters orientation processing in the human lateral geniculate nucleus. *Nature Neuroscience*, *18*(4), 496–498.
- Liu, R. C., Tzovev, S., Rebrik, S., & Miller, K. D. (2001). Variability and information in a neural code of the cat lateral geniculate nucleus. *Journal of Neurophysiology*, *86*, 2789–2806.
- Marrocco, R. T., McClurkin, J. W., & Alkire, M. T. (1996). The influence of the visual cortex on the spatiotemporal response properties of lateral geniculate nucleus cells. *Brain Research*, *737*(1–2), 110–118.
- Maunsell, J. H. R., & Cook, E. P. (2002). The role of attention in visual processing. *Phil. Trans. Royal Society London*, *357*, 1063–1072.
- McAlonan, K., Cavanaugh, J. R., & Wurtz, R. H. (2008). Guarding the gateway to cortex with attention in visual thalamus. *Nature*, *456*, 391–394.
- McClurkin, J. W., Gawne, T. J., Optican, L. M., & Richmond, B. J. (1991). Lateral geniculate neurons in behaving primates. II. Encoding of visual information in the temporal shape of the response. *J. Neurophysiology*, *66*(3), 794–808.
- McClurkin, J. W., Optican, L. M., & Richmond, B. J. (1994). Cortical feedback increases visual information transmitted by monkey parvocellular lateral geniculate nucleus neurons. *Visual Neuroscience*, *11*(3), 601–617.
- Mitchell, J. F., Sundberg, K. A., & Reynolds, J. H. (2009). Spatial attention decorrelates intrinsic activity fluctuations in macaque area V4. *Neuron*, *63*, 879–888.
- Mock, V. L., Luke, K. L., Hembrook-Short, J. R., & Briggs, F. (2018). Dynamic communication of attention signals between the LGN and V1. *Journal of Neurophysiology*, *120*(4), 1625–1639.
- Nover, H., Anderson, C. H., & DeAngelis, G. C. (2005). A logarithmic, scale-invariant representation of speed in macaque middle temporal area accounts for speed discrimination performance. *The Journal of Neuroscience*, *25*(43), 10049–10060.
- O'Connor, D. H., Fukui, M. M., Pinsk, M. A., & Kastner, S. (2002). Attention modulates responses in the human lateral geniculate nucleus. *Nature Neuroscience*, *5*(11), 1203–1209.
- Pouget, A., Zhang, K., Deneve, S., & Latham, P. E. (1998). Statistically efficient estimation using population coding. *Neural Computation*, *10*, 373–401.
- Pryluk, R., Kfir, Y., Gelbard-Sagiv, H., Fried, I., & Paz, R. (2019). A tradeoff in the neural code across regions and species. *Cell*, *176*, 597–609.
- Przybylski, A. W., Gaska, J. P., Foote, W., & Pollen, D. A. (2000). Striate cortex increases contrast gain of macaque LGN neurons. *Visual Neuroscience*, *17*, 485–494.
- Rabinowitz, N. C., Goris, R. L. T., Cohen, M. R., & Simoncelli, E. P. (2015). Attention stabilizes the shared gain of V4 populations. *eLife*, *4*, 1–24, doi:<https://doi.org/10.7554/eLife.08998>.
- Rathbun, D. L., Warland, D. K., & Usrey, W. M. (2010). Spike timing and information transmission at retinogeniculate synapses. *Journal of Neuroscience*, *30*(41), 13558–13566.
- Reinagel, P., & Reid, R. C. (2000). Temporal coding of visual information in the thalamus. *The Journal of Neuroscience*, *20*(14), 5392–5400.
- Seung, H. S., & Sompolinsky, H. (1993). Simple models for reading neuronal population codes. *Proceedings of the National Academy of Science USA*, *90*, 10749–10753.

- Sherman, S. M., & Guillery, R. W. (1998). On the actions that one nerve cell can have on another: Distinguishing "drivers" from "modulators". *PNAS*, *95*, 7121–7126.
- Sherman, S. M., & Guillery, R. W. (2006). *Exploring the thalamus and its role in cortical function* (2nd ed.). Boston: MIT Press.
- Sherman, S. M., & Spear, P. D. (1982). Organization of visual pathways in normal and visually deprived cats. *Physiological Reviews*, *62*(2), 738–850.
- Steriade, M. (2003). The corticothalamic system in sleep. *Frontiers in Bioscience*, *8*, d878–d899.
- Strong, S. P., Koberle, R., de Ruyter van Steveninck, R. R., & Bialek, W. (1998). Entropy and information in neural spike trains. *Physical Review Letters*, *80*(1), 197–200.
- Tsumoto, T., Creutzfeldt, O. D., & Legendy, C. R. (1978). Functional organization of the corticofugal system from visual cortex to lateral geniculate nucleus in the cat. *Experimental Brain Research*, *32*, 345–364.
- Usrey, W. M., Reppas, J. B., & Reid, R. C. (1999). Specificity and strength of retinogeniculate connections. *Journal of Neurophysiology*, *82*, 3527–3540.
- Vanduffel, W., Tootell, R. B. H., & Orban, G. (2000). Attention-dependent suppression of metabolic activity in the early stages of the macaque visual system. *Cerebral Cortex*, *10*, 109–126.

**Publisher's note** Springer Nature remains neutral with regard to jurisdictional claims in published maps and institutional affiliations.